# Cable Nets with Elastically Deformable Edge Ring

**Isabella Vassilopoulou[1] and Charis J. Gantes[2]**

[1] PhD Student, Metal Structures Laboratory, School of Civil Engineering, National Technical University of Athens, Greece
Email address: isabella@central.ntua.gr
[2] Assistant Professor, Metal Structures Laboratory, School of Civil Engineering, National Technical University of Athens, Greece
Email address: chgantes@central.ntua.gr
Postage Address: PO Box 31830, GR-10035, Athens, Greece

(Received 7th February 2005)

**ABSTRACT:** The objective of this work is to present the behavior of prestressed cable net structures anchored to an elastically deformable edge ring and to propose a methodology for their preliminary analysis and design. The interaction between the edge ring and the cable net is examined. The proposed method for preliminary analysis and design is based on charts, produced via geometrically nonlinear analysis for a structure with specific geometrical and mechanical characteristics, and suitable transformation relations. Using them, it is possible to calculate the maximum tension and deflection of the cables and the maximum internal forces, moments and deformations of the edge ring, for any cable net with similar geometry. The charts presented in this paper cover nets with circular plan view. Nevertheless, the methodology can be readily extended to other shapes.

**Key Words**: cable net, elastically deformable edge ring, geometrically nonlinear analysis, preliminary design, charts

## 1 INTRODUCTION

The capacity of cable net roofs to cover long spans without intermediate supports and to carry large loads, much larger than their self-weight, stimulated the interest of engineers and architects in the sixties. The demand for this kind of structures increased after the evolution of computers and the development of numerical methods for solving large systems of nonlinear equations. These structures are very stable and efficient, since the loads are transmitted through tension of the cables, usually made of high-strength steel, having thus the best exploitation of the material. Moreover, with their unusual forms they differ from all other, conventional structures, something that makes them extremely elegant. Cable net roofs are used to cover stadiums, swimming pools, ice rinks, exhibition halls, theatres, hangars, or even factories.

An infinite number of shapes can be produced by pretensioned cable net roofs, that depend on the geometry of their boundaries, the curvatures, the levels of cable pretension and the eventual internal supports. They usually have a rectangular, rhomboid, circular or elliptical plan and the shape of their surface is that of a hyperbolic paraboloid, where the two opposite boundary edges are higher than the other two. In this way, different curvatures develop in two perpendicular directions, that enable prestressing, thus rendering the system stiffer. The cables are anchored to an edge ring, usually made of prestressed concrete and having a closed box cross-section, that is elastically deformable but much stiffer than the cables. The cables that are anchored to the highest points of the edge ring are called primary or carrying cables and those that are anchored to the lowest points are called secondary or stabilizing cables (Fig. 1).

The geometry of the net is defined by the equation of the hyperbolic paraboloid surface, which is:

$$z = \frac{k_x}{2} x^2 - \frac{k_y}{2} y^2 \tag{1}$$

where,

$$k_x = \frac{8f_x}{L_x^2},\ k_y = \frac{8f_y}{L_y^2} \tag{2}$$

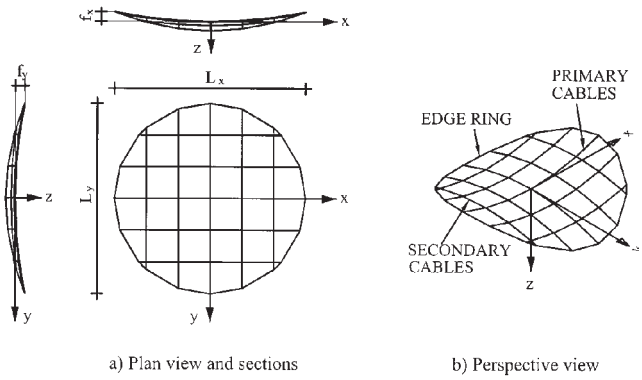


a) Plan view and sections b) Perspective view

Figure 1. Cable net of hyperbolic paraboloid shape with elliptical plan

are the curvatures, and $f_x$, $f_y$ are the sags, considered always positive. For the case of elliptical plan the equation of the horizontal projection of the edge is:

$$\frac{4}{L_x^2}x^2 + \frac{4}{L_y^2}y^2 = 1 \tag{3}$$

The stiffness of the system is achieved as a result of the opposite curvatures of the surface, the cross-section and the pretension of the cables and the stiffness of the boundary. In this kind of structures, large deformations occur, mainly because, due to their lack of shear rigidity, the cables change their shape in order to equilibrate the loads without shear.

The large deflections can be alleviated by appropriate level of pretension, which should be such that, under any load combination, the cables remain in tension and never become slack. Flat or nearly flat regions of the cable net surface should be avoided because their stiffness is insufficient and they may easily flutter (Buchholdt[1]).

In general, however, the suspended roofs cannot be calculated on the basis of linear theory, due to the large deformations that occur and the associated difference between their undeformed and their deformed shape. Thus, their analysis should be geometrically nonlinear (Vilnay[2] and Broughton and Ndumbaro[3]). Because of this nonlinear behavior, the design of such structures is complicated, since the principle of superposition does not apply and separate nonlinear analyses must be performed for each loading combination (Szabó et al.[4]). The available analysis methods for this kind of tensile structures are presented thoroughly by Majowiecki[5].

Due to the computational effort required in order to perform a large number of nonlinear analyses, it would be very useful to have preliminary design guidelines, enabling the engineers to make a better choice of the distance between cables, of their cross-sections and of the level of pretension, and thus have a first estimate of the cost of the structure. A first attempt of a preliminary analysis of cable network structures has been introduced by Gero[6, 7]. This method is restricted to nets with fixed cable edges, neglecting the deformation of the edge ring, which is considered rigid. The method is based on the transformation of a network with large number of cables, called prototype, to a smaller network, that has a geometry similar to the prototype, referred to as model, using transformation relations and charts, that have been produced with geometrically nonlinear analyses. The two networks, the prototype and the model, must have similar geometry, so that their corresponding quantities can also be similar. The charts describe the behavior of the model, namely the maximum tension of the cables and the maximum deflections of the net. By using the transverse transformation relations we can evaluate the behavior of the prototype. This method is based on the Buckingham Pi theorem (Giles[8]).

However, the deformability of the edge ring causes a variation in the tension of the cables and in the deflection of the net. A mathematical model for the analysis of such systems is presented by Talvik[9] and Majowiecki and Zoulas[10]. Szabó et al.[4] propose another method of preliminary analysis of cable nets with elliptical plan, that takes into consideration the effect of the closed edge ring on the response of the net. This method is developed in two steps: a) The edge ring is presumed infinitely rigid and consequently undeformed, and the problem is solved only for the cable force distribution that causes compression to the ring, b) The edge ring is presumed deformable and the problem is solved only for the cable force distribution that causes bending to the ring. However, this method does not take into account the change of the geometry of the cables, thus, the calculations are based on the undeformed structure. The influence of the deformations may be considered by repeating the process, taking the changed shape as a basis for the next iteration.

The aim of the present paper is to extend the preliminary design method developed by Gero[6, 7] to elastically supported cable network structures, by taking into account the characteristics of the edge ring, and more specifically its flexural stiffness $E_rI_r$. Thus, the ring is no longer considered rigid, but elastically deformable, accounting for more realistic boundary conditions for the cables. In addition, the response of the edge ring is delineated by diagrams of the internal

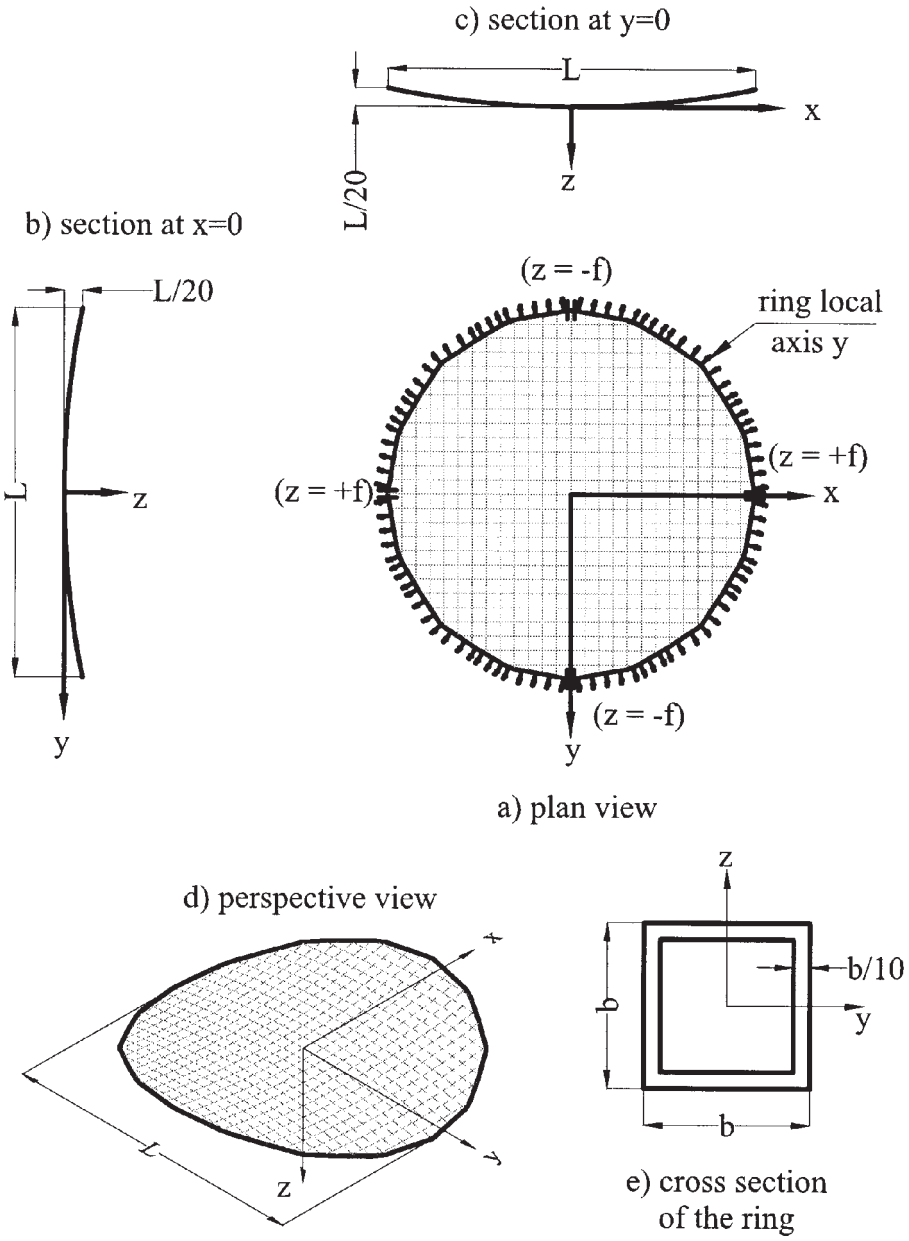


Figure 2. Geometry of the net adopted for the nonlinear analysis

forces and its deformation. A parametric nonlinear analysis is carried out for different values of stiffness of the cables (EA) and that of the ring ($E_rI_r$), and different values of pretension and nodal loads, in order to examine the behavior of the system. The present work examines also the effect of the curvature of the net in the behaviour of the system and provides additional charts and transformation relations for the preliminary design of the edge ring, including the sag-to-span ratio of the net as a variable in the transformation relations. Consequently, it is possible to calculate the maximum tension and deflection of the cables and the maximum internal forces, moments and deformations of the boundary beam, for any cable net with similar geometry to the model, even if it has a different sag-to-span ratio from the latter.

The accuracy of the proposed methodology is illustrated for two specific numerical examples.

## 2 MODELING ISSUES

The cable net adopted for this study is geometrically defined as a hyperbolic paraboloid surface with a circular plan view of diameter L (Fig. 2). The net consists of N cables in each direction with circular cross-section of area A and diameter D. The edge ring has a square box section of width b, wall thickness

b/10, area $A_r$ and moment of inertia $I_r$. The elastic modulus of the cables is E and that of the edge ring $E_r$. For the analysis, the edge ring is modeled by beam elements and the cables by cable elements, that can only sustain tension. Each part of a cable between two adjacent net intersection points is modeled with one cable element.

The geometrically nonlinear analysis is performed with the finite element software SOFiSTiK[11]. The model is a 3-dimensional structure and the z-displacement of the nodes of the edge ring are restrained. The deformation in the x-direction is not permitted for the two nodes of the ring with coordinate y=0, and, respectively, the y-deformation is not permitted for the two nodes of the ring with coordinate x=0, in order to avoid rigid body motion.

The following assumptions are made: (i) the cable material is linearly elastic, (ii) the loads are applied on the nodes, (iii) the boundary of the cables can be considered either fixed or elastic (if they are anchored to an elastic edge ring), (iv) the structure is uniformly loaded and uniformly prestressed, (v) all cables are arranged in a grid of equal distances, (vi) all cables have the same cross-section and elastic modulus, (vii) the cables can sustain only tension, and (viii) the analysis is geometrically nonlinear taking into account the axial deformation of the cables.

## 3 THE BEHAVIOR OF THE SYSTEM

When the cable net is loaded with downward vertical load, the tension of the primary cables increases, whilst the tension of the secondary cables decreases. Thus, in the deformed structure the high points of the edge ring are approaching each other and the low points are moving away from each other (Fig. 3). When the edges of the cables are not fixed but anchored to an elastic edge ring, the deflections are larger and the cable tensions are smaller, because the system is less stiff. The tension along the cables increases towards the edges of the cable, because its horizontal component remains constant, while its vertical component increases to equilibrate the increased shear force due to the vertical load applied to the nodes. If the load is very small with respect to the pretension of the cables, the increment of the tension towards their edges is also very small. Due to the loading of the net the edge ring is subjected to compression, shearing and bending. The primary mode of action of the edge ring is axial compression N, but in addition, because of the geometry of the boundary, that is not plane, shear forces $Q_y$ and $Q_z$ and bending moments $M_y$ and $M_z$, referring to the local axes of the ring (Fig. 2), are observed. The internal forces of the ring are shown in Figure 4, and some representative tensions of the cables in Figure 5, where it is confirmed that the tensions of the primary cables are larger than those of the secondary cables. In Figure 6 the load-deflection diagram is presented, confirming the nonlinear behavior of the net, that becomes stiffer as the external load increases.

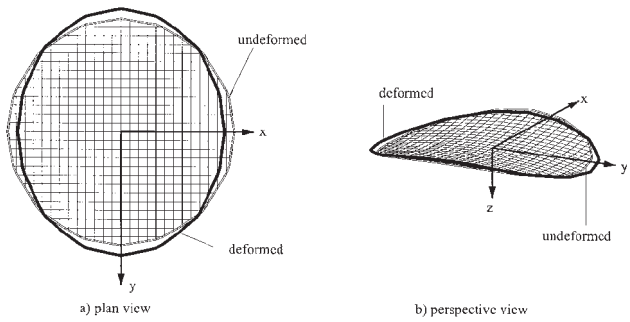


Figure 3. The deformed structure

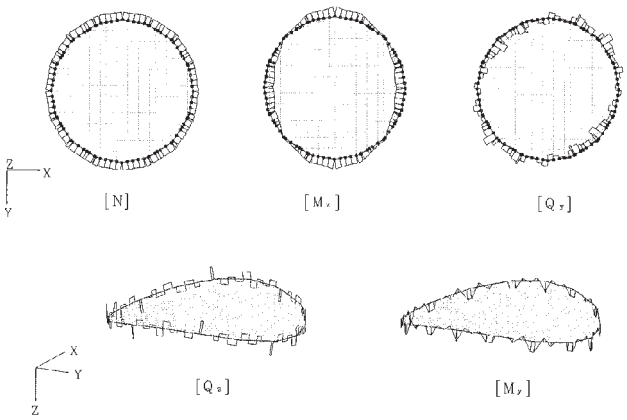


Figure 4. Internal forces of the edge ring

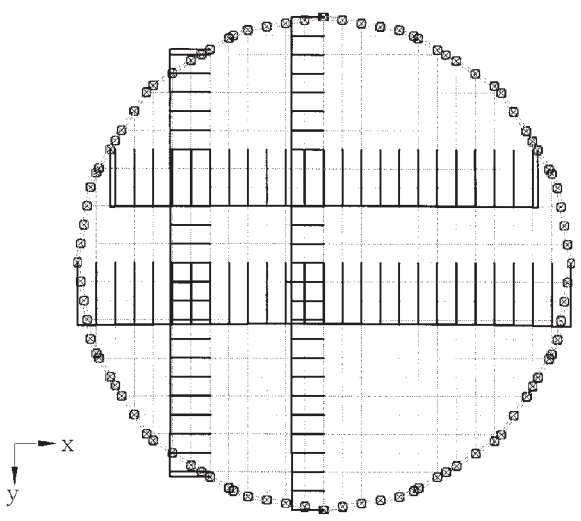

Figure 5. Cable tensions

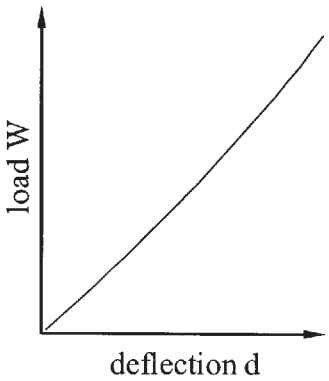


Figure 6. The nonlinear behavior of the net

## 4 PARAMETRIC ANALYSES

The cable net adopted for the parametric analyses is geometrically defined by a hyperbolic paraboloid surface with a circular plan view of 100m diameter, and sags $f_x$=$f_y$=5m, described by the equations:

$$z = \frac{5}{50^2}(x^2 - y^2) \quad \text{: equation of the surface} \quad (4)$$

$$x^2 + y^2 = 50^2 \quad \text{: equation of the horizontal projection of the edge} \quad (5)$$

It consists of a net of 25 cables in each direction. The elastic modulus of the cables is E=200,000MPa and that of the edge ring $E_r$=34,000MPa. The cable diameter is D=20mm and the width of the edge cross section is b=6.00m.

In this section the results of some parametric analyses are presented, in order to provide insight into the behavior of the system. Figure 7 illustrates the effect of load and pretension on the maximum cable tension, maximum net deflection and the maximum internal forces of the edge ring referring to the local axes of the ring. In Figure 8 the effect of cable and ring stiffness on the same quantities are presented.

From these graphs important conclusions can be drawn regarding the cable net's behavior. More specifically, it is noted that:

- The nonlinear behavior of the cables causes a nonlinear response on the edge ring.
- The behavior of the structure becomes stiffer and less nonlinear for increasing levels of loading.
- The system responds in a stiffer and less nonlinear manner as the pretension increases.
- The shear and bending of the ring decrease and its compression increases as pretension increases.
- As the stiffness of the edge ring increases the deflection of the net decreases because the boundary becomes stiffer. The internal forces of the ring also increase except of the maximum shear force $Q_z$ that arrives to a pick and then decreases.
- As the stiffness of the cables increases the maximum values of the internal forces of the ring increase; on the other hand, the maximum deflection of the net decreases and the tensions of the cables increase because the net becomes stiffer.

For low values of the ring stiffness, the tension of the secondary cables, that is supposed to decrease, becomes zero and tends to increase, its curvature changes direction and the system is no longer stiff, as also explained by Majowiecki[5] and Majowiecki and Zoulas[10].

The same model but for different sag values f=L/20, L/25 and L/30 is used in order to provide insight into the behavior of the system due to the sag of the cables. Figure 9 illustrates the effect of sag and nodal load on the maximum cable tension T, the maximum net deflection $d_z$, the maximum internal forces of the edge ring $N_x$, $Q_y$, $M_z$, referring to the local axes of the ring, and the maximum deformations of the edge ring $d_x$ and $d_y$, for a range of values of the nodal load between 1kN and 20kN. Each point on the charts refers to a load step of 1kN. From these graphs it is noted that:

- The system responds in a stiffer and less nonlinear manner as the sag-to-span ratio increases.
- The difference in maximum cable tension and ring internal forces for the same nodal load as the sag-to-span ratio changes, is not significant in relation to the magnitude of these forces.

## 5 SCALING RELATIONSHIPS

The method proposed by Gero[6, 7] for the scaling of the prototype to the model with fixed cable edges, is based on the Buckingham Pi theorem, which is a key theorem in dimensional analysis (Wikipedia[12]).

The Buckingham Pi theorem states that the functional dependence between a certain number (e.g.: n) of variables can be reduced by the number (e.g. k) of independent dimensions occurring in those variables to give a set of p = n – k independent, dimensionless numbers. It provides a method for computing sets of dimensionless parameters from the given variables. However, the choice of dimensionless parameters is not unique. Examples of this theorem are given by Shih[13].

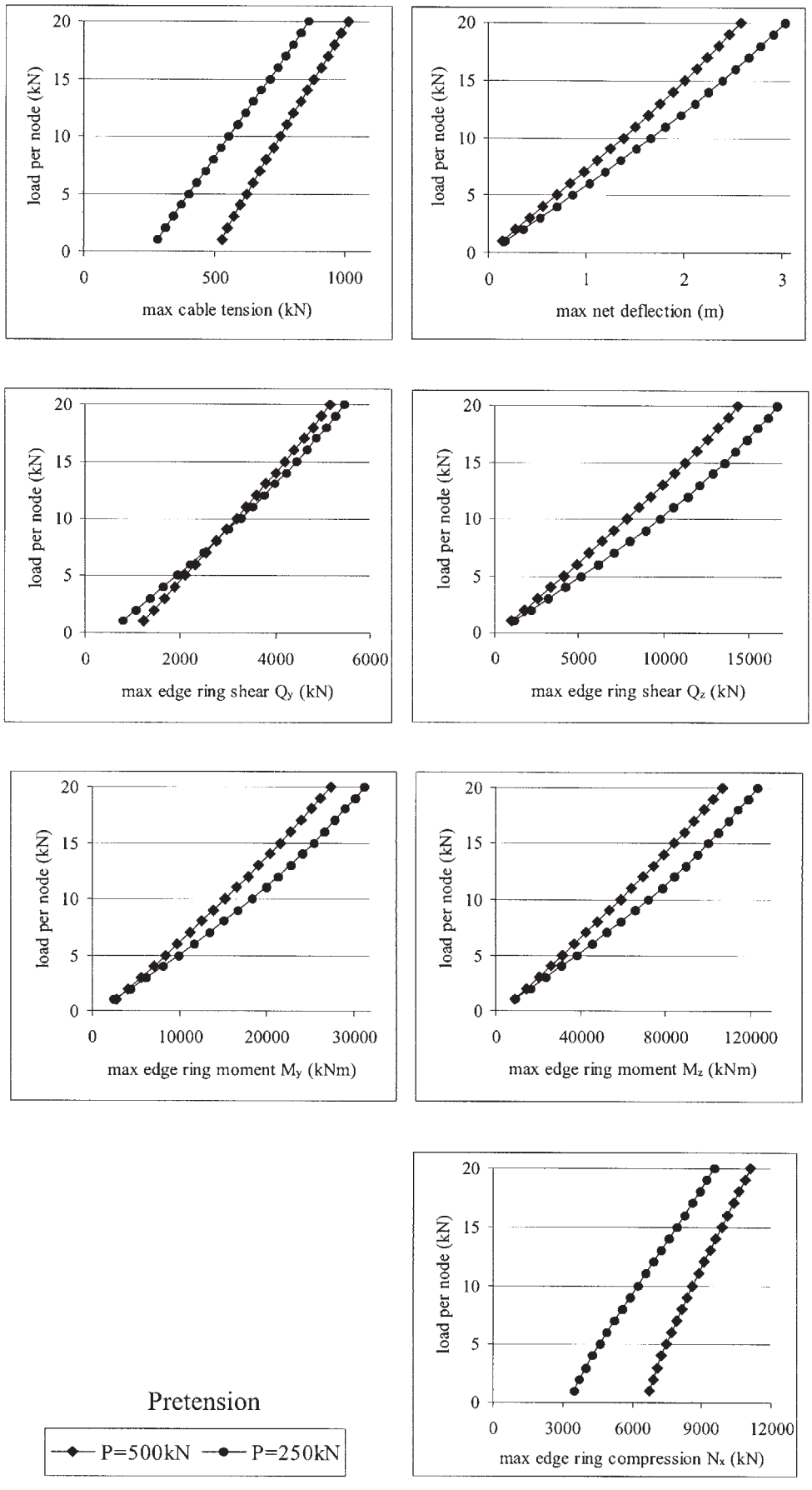


Figure 7. The effect of the various levels of pretension and load on the response

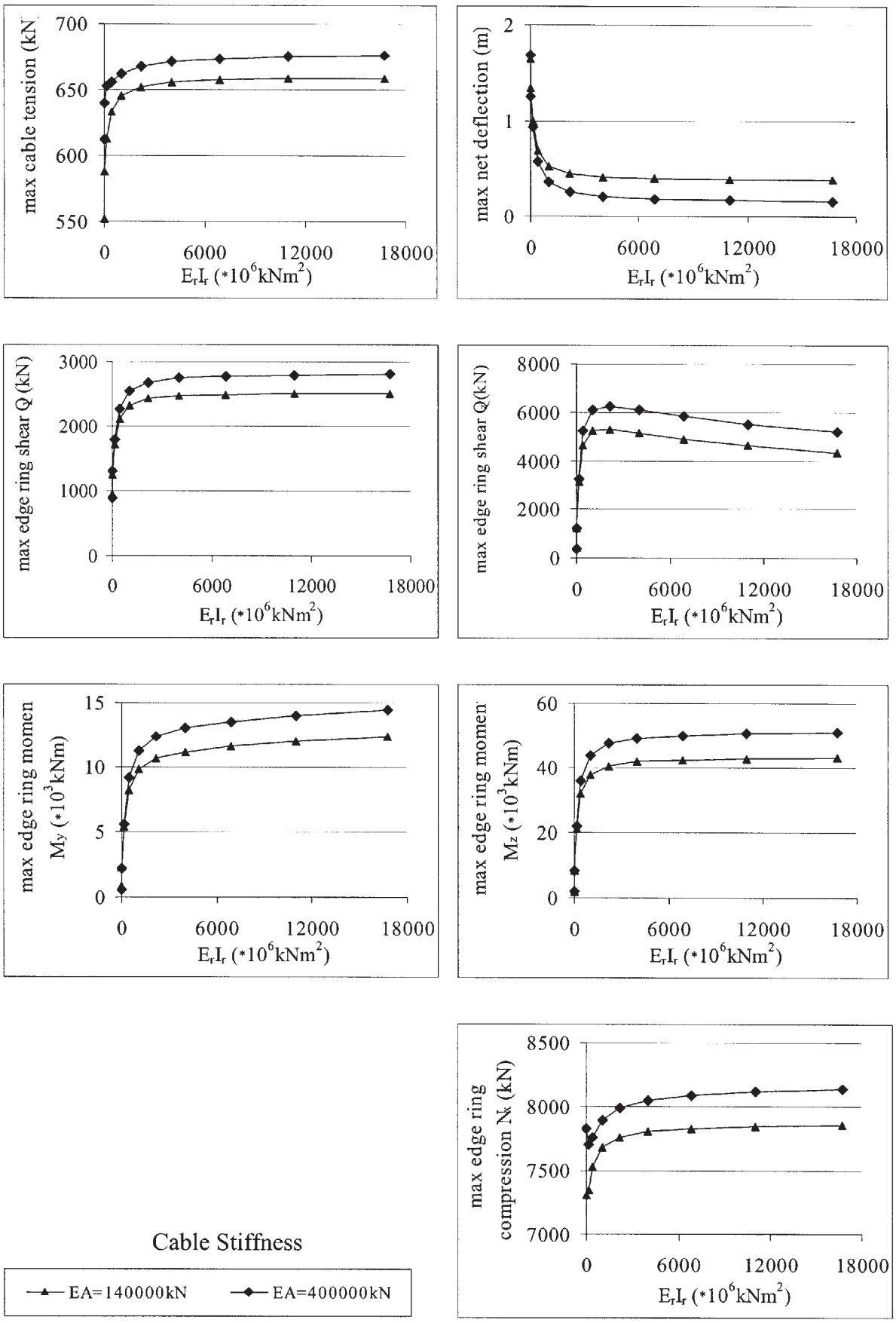


Figure 8. The effect of the stiffness of the cables and the stiffness of the edge ring on the response

The transformation relations proposed by Gero[6, 7] for cable networks, are the following:

$$W_m = W_p \left(\frac{E_m}{E_p}\right)\left(\frac{L_m}{L_p}\right)^2\left(\frac{N_p}{N_m}\right)^2$$

: nodal loads (6)

$$A_m = A_p \left(\frac{L_m}{L_p}\right)^2\left(\frac{N_p}{N_m}\right)$$

: cable cross sectional area (7)

$$(EA)_m = (EA)_p \left(\frac{E_m}{E_p}\right)\left(\frac{L_m}{L_p}\right)^2\left(\frac{N_p}{N_m}\right)$$

: cable axial stiffness (8)

$$P_m = P_p \left(\frac{E_m}{E_p}\right)\left(\frac{L_m}{L_p}\right)^2\left(\frac{N_p}{N_m}\right)$$

: cable pretension (9)

$$T_m = T_p \left(\frac{E_m}{E_p}\right)\left(\frac{L_m}{L_p}\right)^2\left(\frac{N_p}{N_m}\right)$$

: cable tension (10)

$$d_m = d_p \frac{L_m}{L_p}$$

: nodal deflections (11)

where N is the number of the cables per direction, L is the maximum length of the cables, E the elastic modulus of the cables, while m and p are subscripts referring to model and prototype, respectively.

The accuracy of these transformation relations has been examined by the authors through the results they give for different ratios of number of cables prototype and model, ranging between $N_p/N_m = 5/3 = 1.667$ and $N_p/N_m = 9/3 = 6.333$. The accuracy for tensions is within +12% and for deflections +35%. However, in the course of our effort to obtain transformation relations accounting also for the edge ring, we found that, by replacing the ratio $N_p/N_m$ with the ratio $(N_p+1)/(N_m+1)$ the accuracy for tensions reaches –2% and for deflections +8%. This is attributed to the fact that the ratio L/(N+1) stands for the distance between the cables, while the ratio L/N has no physical meaning. Thus, the improved transformation relations that take into consideration the elastic supports of the cables to the elastically deformable edge ring (Vassilopoulou and Gantes[14]), as well as the new transformation relations regarding the internal forces

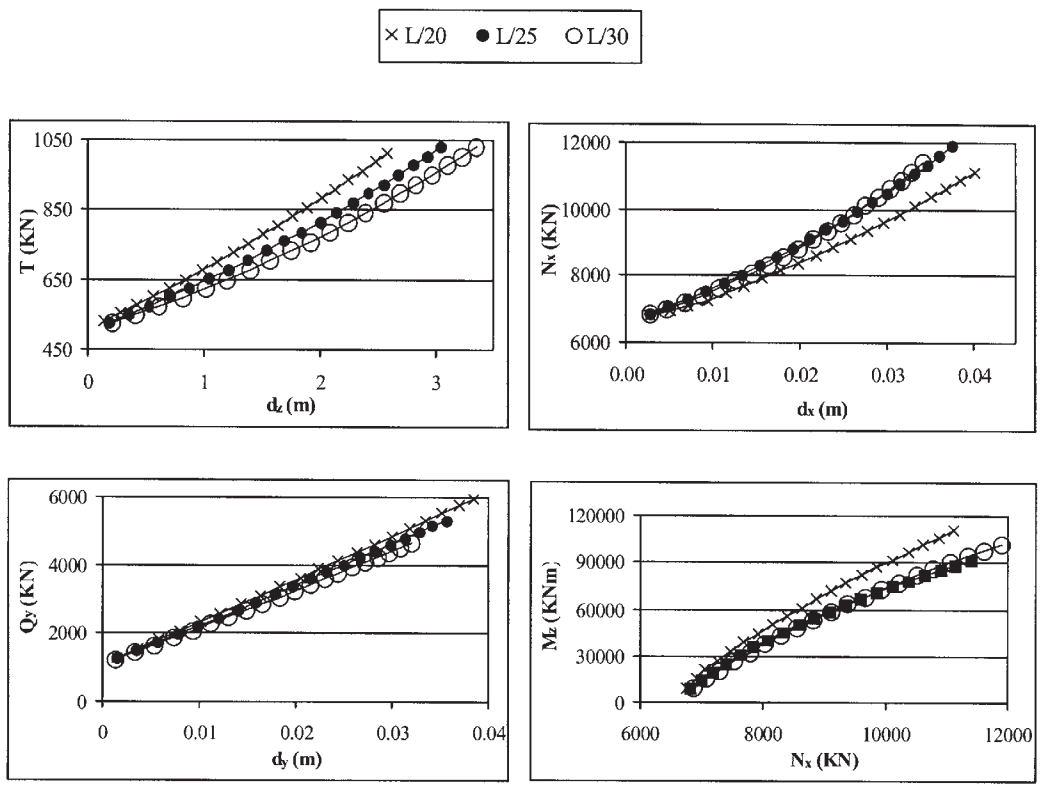


Figure 9. The effect of various sag-to-span ratios on the response of a network, for nodal loads 1–20kN

and the deformations of the edge ring, and the effect of the curvature in the behavior of the system, are the following (Vassilopoulou and Gantes[15]):

$$W_m = W_p \left(\frac{E_m}{E_p}\right)\left(\frac{(E_r)_m}{(E_r)_p}\right)\left(\frac{L_m}{L_p}\right)^2 \left(\frac{N_p+1}{N_m+1}\right)^2 \sqrt{\frac{f_m/L_m}{f_p/L_p}}$$

: nodal loads (12)

$$D_m = D_p \left(\frac{L_m}{L_p}\right)\sqrt{\left(\frac{N_p+1}{N_m+1}\right)\left(\frac{(E_r)_m}{(E_r)_p}\right)}\left(\frac{f_p/L_p}{f_m/L_m}\right)$$

: cable diameter (13)

$$A_m = A_p \left(\frac{L_m}{L_p}\right)^2 \left(\frac{N_p+1}{N_m+1}\right)\left(\frac{(E_r)_m}{(E_r)_p}\right)\left(\frac{f_p/L_p}{f_m/L_m}\right)^2$$

: cable cross sectional area (14)

$$(EA)_m = (EA)_p \left(\frac{E_m}{E_p}\right)\left(\frac{(E_r)_m}{(E_r)_p}\right)\left(\frac{L_m}{L_p}\right)^2 \left(\frac{N_p+1}{N_m+1}\right)\left(\frac{f_p/L_p}{f_m/L_m}\right)^2$$

: cable axial stiffness (15)

$$P_m = P_p \left(\frac{E_m}{E_p}\right)\left(\frac{(E_r)_m}{(E_r)_p}\right)\left(\frac{L_m}{L_p}\right)^2 \left(\frac{N_p+1}{N_m+1}\right)$$

: cable pretension (16)

$$T_m = T_p \left(\frac{E_m}{E_p}\right)\left(\frac{(E_r)_m}{(E_r)_p}\right)\left(\frac{L_m}{L_p}\right)^2 \left(\frac{N_p+1}{N_m+1}\right)$$

: cable tension (17)

$$d_m = d_p \frac{L_m}{L_p}$$

: nodal deflections (18)

$$b_m = b_p \left(\frac{L_m}{L_p}\right)\sqrt[4]{\left(\frac{E_m}{E_p}\right)}$$

: ring cross section width (19)

$$(I_c)_m = (I_c)_p \left(\frac{E_m}{E_p}\right)\left(\frac{L_m}{L_p}\right)^4$$

: ring moment of inertia (20)

$$(E_r I_r)_m = (E_r I_r)_p \left(\frac{E_m}{E_p}\right)\left(\frac{(E_r)_m}{(E_r)_p}\right)\left(\frac{L_m}{L_p}\right)^4$$

: ring flexural stiffness (21)

$$(N_x)_m = (N)_p \left(\frac{E_m}{E_p}\right)\left(\frac{(E_r)_m}{(E_r)_p}\right)\left(\frac{L_m}{L_p}\right)^2$$

: ring normal force (22)

$$(Q_y)_m = (Q_y)_p \left(\frac{E_m}{E_p}\right)\left(\frac{(E_r)_m}{(E_r)_p}\right)\left(\frac{L_m}{L_p}\right)^2$$

: ring shear force (23)

$$(M_z)_m = (M_z)_p \left(\frac{E_m}{E_p}\right)\left(\frac{(E_r)_m}{(E_r)_p}\right)\left(\frac{L_m}{L_p}\right)^3$$

: ring bending moment (24)

$$(d_r)_m = (d_r)_p \frac{L_m}{L_p}$$

: ring deformation (25)

The accuracy obtained by using these transformation relations depends on the ratio of the numbers of cables in model and prototype. Tables 1, 2 and 3 show the results from different analyses, based on a prototype of 25 cables, and several models with 3, 5, 7, 11, 19, 35 cables, and keeping the parameters L, f, E and $E_rI_r$ unchanged in both prototype and model. The accuracy for tensions is within –4.1% while the accuracy for deflections is within +6.4%.

## 6 PRELIMINARY DESIGN CHARTS

The model adopted for the production of the charts is the one described in section 4 for L=100m and f=L/20. The cross-section diameter of all cables varies between 25mm and 50mm, in order to have a range of cable stiffness between the values EA = 100,000 ~ 400,000kN. Likewise, the edge ring has a section width b that varies between 4.95m and 7.40m, so that the range of ring stiffness is between the values $E_rI_r$ = 1,000,000,000kNm$^2$ and 5,000,000,000kNm$^2$. This cable net roof has been chosen as the model, because its characteristics resemble those of a typical real structure, so that the results derived from the proposed method will be more accurate.

The charts produced are dimensionless and can be used for every system of units. They provide the maximum tensions and maximum deflections of the net (Figs. 10, 11), the maximum internal forces and the maximum deformations of the edge ring (Figs. 12–17) for this model for the following values of stiffness of cables and edge ring, pretension and loads:

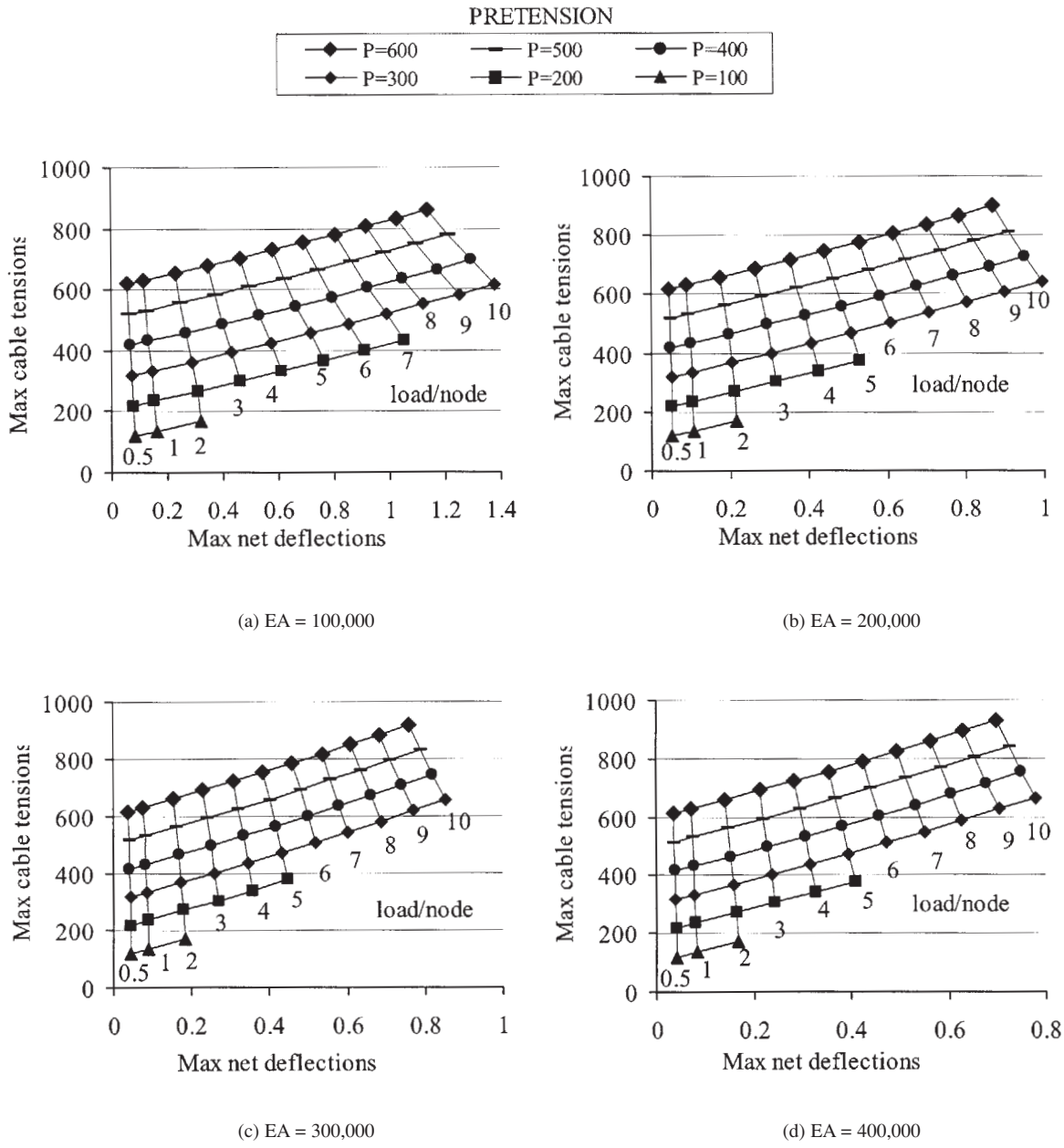


(a) EA = 100,000

(b) EA = 200,000

(c) EA = 300,000

(d) EA = 400,000

Figure 10. Charts of cable tension and net deflection for pretension P = 100–600, load per node W = 0.5–10, ring stiffness $E_rI_r$ = 1,000,000,000, cable stiffness EA = 100,000 ~ 400,000

EA = 100,000 ~ 400,000,
$E_rI_r$ = 1,000,000,000 ~ 5,000,000,000,
P = 100 ~ 600,
W = 0.5 ~ 10

Comparing the charts in Figure 10 and those in Figure 11 it can easily be noted that the influence of the ring flexural stiffness on the maximum tension of the cables is not very large, but the difference in the corresponding deflections of the net is substantial.

When the load counterbalances the pretension, the tension of the secondary cables becomes zero and the net is no longer stable. This occurs if the load is large compared to the pretension. If we use the values of tensions and deflections after the elimination of the tension in some cables, this method gives inaccurate results, as explained by Vassilopoulou[16] and confirmed by our analyses. The above charts provide satisfactory values for the tension of the cables and deflection of the net, before this phenomenon takes place, that is, the curves stop for the combination of the load and pretension which eliminates the tension of the secondary cables.

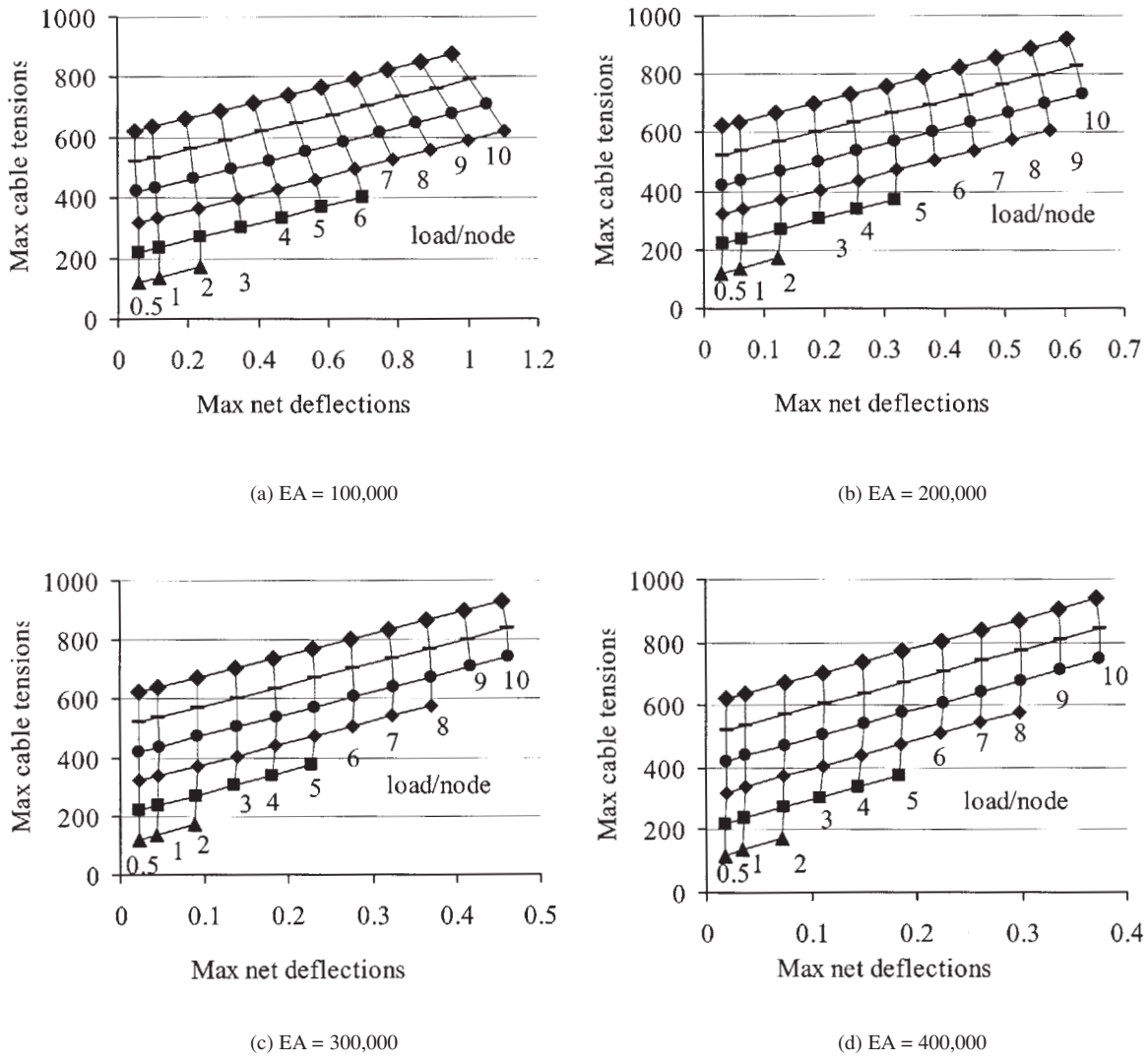


Figure 11. Charts of cable tension and net deflection for pretension P = 100–600, load per node W = 0.5–10, ring stiffness $E_rI_r$ = 5,000,000,000, cable stiffness EA = 100,000 ~ 400,000

## 7 EXAMPLE 1

In order to comprehend the proposed method and to verify its accuracy two examples are provided. For the first example the prototype is a cable net with the characteristics given in Table 4. The units that are used are 'kN' for forces and 'm' for length.

Using 'eqns (12–25)' these prototype parameters can be scaled to the model, for which the above charts have been produced. Therefore:

$$\frac{L_m}{L_p}=\frac{100}{180}=0.555 \qquad \frac{N_p+1}{N_m+1}=\frac{35+1}{25+1}=1.385$$

$$\frac{E_m}{E_p}=\frac{200{,}000{,}000}{200{,}000{,}000}=1 \qquad \frac{(E_r)_m}{(E_r)_p}=\frac{34{,}000{,}000}{34{,}000{,}000}=1$$

$W_m = W_p*1*1*0.555^2*1.385^2 = W_p*0.59 = 7*0.59 = 4.13$kN/node

$D_m = 0.070*0.555*(1.385*1)^{1/2} = 0.04572$m

$A_m = 0.003848*0.555^2*1.385*1 = 0.00164$m$^2$

$(EA)_m = 770{,}000*1*1*0.555^2*1.385 = 33{,}000$kN

$P_m = 800*1*1*0.555^2*1.385 = 341$kN

$(T_u)_m = 1{,}800*1*1*0.555^2*1.385 = 768$kN

$b_m = 10*0.555*(1)^{1/4} = 5.55$m

$(I_r)_m = 492*0.555^4*1 = 46.68$m$^4$

**Table 1. Accuracy of tensions and deflections for different number of cables and load $W_m$ = 1kN/node**

| | Number of cables | Load $W_m$=1kN/node | Error $(T–T_p)/T_p$ $(d–d_p)/d_p$ |
|---|---|---|---|
| **Prototype** | **$N_p$=25** | **$T_p$=131.63kN $d_p$=0.251m** | |
| Model | $N_m$=3 | T=126.47kN d=0.267m | –3.9% 6.4% |
| Model | $N_m$=5 | T=127.08kN d=0.264m | –3.5% 5.1% |
| Model | $N_m$=7 | T=129.04kN d=0.257m | –2.0% 2.4% |
| Model | $N_m$=11 | T=130.08kN d=0.253m | –1.2% 0.8% |
| Model | $N_m$=19 | T=131.39kN d=0.252m | –0.2% 0.4% |
| Model | $N_m$=35 | T=131.80kN d=0.250m | +0.1% –0.4% |

**Table 2. Accuracy of tensions and deflections for different number of cables and load $W_m$ = 2kN/node**

| | Number of cables | Load $W_m$=2kN/node | Error $(T–T_p)/T_p$ $(d–d_p)/d_p$ |
|---|---|---|---|
| **Prototype** | **$N_p$=25** | **$T_p$=168.55kN $d_p$=0.2484m** | |
| Model | $N_m$=3 | T=162.01kN d=0.510m | –3.9% 5.4% |
| Model | $N_m$=5 | T=161.75kN d=0.507m | –4.0% 4.8% |
| Model | $N_m$=7 | T=164.84kN d=0.494m | –2.2% 2.1% |
| Model | $N_m$=11 | T=166.22kN d=0.487m | –1.4% 0.6% |
| Model | $N_m$=19 | T=168.18kN d=0.485m | –0.2% 0.2% |
| Model | $N_m$=35 | T=168.80kN d=0.483m | 0.1% –0.4% |

**Table 3. Accuracy of tensions and deflections for different number of cables and load $W_m$ = 3kN/node**

| | Number of cables | Load $W_m$=3kN/node | Error $(T–T_p)/T_p$ $(d–d_p)/d_p$ |
|---|---|---|---|
| **Prototype** | **$N_p$=25** | **$T_p$=207.66kN $d_p$=0.691m** | |
| Model | $N_m$=3 | T=200.17kN d=0.721m | –3.6% 4.3% |
| Model | $N_m$=5 | T=199.13kN d=0.720m | –4.1% 4.2% |
| Model | $N_m$=7 | T=203.22kN d=0.703m | –4.1% 1.7% |
| Model | $N_m$=11 | T=204.69kN d=0.695m | –1.4% 0.6% |
| Model | $N_m$=19 | T=207.19kN d=0.692m | –0.2% 0.1% |
| Model | $N_m$=35 | T=207.96kN d=0.689m | 0.1% –0.3% |

**Table 4. Characteristics of the prototype – example 1**

| Cables | Edge ring |
|---|---|
| $L_p$ = 180m | b = 10m |
| $N_p$ = 35 cables | $A_r$ = 36m$^2$ |
| $W_p$ = 7.0kN/node | $(I_r)_p$ = 492m$^4$ |
| $D_p$ = 0.070m | $(E_r)_p$ = 34,000,000kNm$^2$ |
| $A_p$ = 0.003848m$^2$ | $(E_rI_r)_p$ = 17,000,000,000kNm$^2$ |
| f = $L_p$/20 = 9m | |
| $E_p$ = 200,000,000kN/m$^2$ | |
| $(EA)_p$ = 770,000kN | |
| $P_p$ = 800kN | |
| $(T_u)_p$ = 1,800KN | |

$(E_rI_r)_m = 17{,}000{,}000{,}000*1*1*0.555^4 = 1{,}600{,}000{,}000\text{kNm}^2$

It is necessary to shift these parameters within the range of the charts. This can be done by setting:

$$E_m = \frac{E}{1.6} = \frac{200{,}000{,}000}{1.6}$$

$$\frac{L_m}{L_p} = \frac{100}{180} = 0.555 \qquad \frac{N_p + 1}{N_m + 1} = \frac{35+1}{25+1} = 1.385$$

$$\frac{E_m}{E_p} = \frac{200{,}000{,}000}{1.6 * 200{,}000{,}000} = \frac{1}{1.6}$$

$$\frac{(E_r)_m}{(E_r)_p} = \frac{34{,}000{,}000}{34{,}000{,}000} = 1$$

$W_m = W_p*(1/1.6)*1*0.555^2*1.385^2 = 2.60$kN/node

$D_m = 0.070*0.555*(1.385*1)^{1/2} = 0.04572$m

$A_m = 0.003848*0.555^2*1.385*1 = 0.00164$m$^2$

$(EA)_m = 770{,}000*(1/1.6)*1*0.555^2*1.385 = 205{,}000$kN

$P_m = 800*(1/1.6)*1*0.555^2*1.385 = 213$kN

$(T_u)_m = 1{,}800*(1/1.6)*1*0.555^2*1.385 = 480$kN

$b_m = 10*0.555*(1/1.6)^{1/4} = 4.93$m

$(I_r)_m = 492*0.555^4*(1/1.6) = 29.18$m$^4$

$(E_rI_r)_m = 17{,}000{,}000{,}000*(1/1.6)*1*0.555^4 = 1{,}000{,}000{,}000$kNm$^2$

For load $W_m$ = 2.60kN/node, stiffness of cables $(EA)_m$ = 200,000kN, pretension of cables $P_m$ = 213kN, and stiffness of the edge ring $(E_rI_r)_m$ = 1,000,000,000kNm$^2$, the values of maximum deflection and maximum tension can be derived from chart b of Figure 10:

$d_m$ = 0.270m : maximum nodal deflection

$T_m$ = 300kN : maximum cable tension

These values can be scaled back to the prototype using the inverse 'eqns (17–18)':

$T_p = 300*1*1.6*1.8^2*0.722 = 1{,}123.2$kN

$d_p = 0.270*1.80 = 0.486$m

The values of maximum deflection and maximum internal forces of the edge ring as well as the maximum ring's deformations can be derived from charts b of Fig. 12, 14 and 16:

$(N_x)_m$ = 3,600kN :maximum ring normal force

$(Q_y)_m$ = 1,325kN :maximum ring shear force

$(M_z)_m$ = 24,870kNm :maximum ring moment

$(d_x)_m$ = 0.020m :maximum ring deformation x

$(d_y)_m$ = 0.019m :maximum ring deformation y

These values can be scaled back to the prototype using the inverse 'eqns (22–25)':

$(N_x)_p = 3{,}600*1*1.6*1.8^2 = 18{,}662.4$kN

$(d_x)_p = 0.020*1.8 = 0.036$m

$(Q_y)_p = 1{,}325*1.6*1.8^2 = 6{,}868.8$kN

$(d_y)_p = 0.019*1.8 = 0.034$m

$(M_z)_p = 24{,}870*1.6*1.8^3 = 232{,}066.94$kNm

Using the program SOFiSTiK and performing an exact nonlinear analysis of the prototype the maximum deflection obtained for the nodes of the net is d=0.486m and the maximum tension of the cables T=1133kN, while the maximum internal forces and deformations obtained for the edge ring are:

$N_x$ = 22,010.88kN

$d_x$ = 0.0355m

$Q_y$ = 7,035.6kN

$d_y$ = 0.0334m

$M_z$ = 230,016.4kNm

The accuracy is 100% for the net deflections, 99.1% for the cable tensions, 84.8% for the ring normal force $N_x$, 97.6% for the ring shear force $Q_y$, 99.1% for the ring moment $M_z$ and 98.6% and 98.2% for the ring deformations $d_x$ and $d_y$, respectively.

**Table 5. Characteristics of the prototype – example 2**

| Cables | Edge ring |
|---|---|
| $L_p$ = 180m | b = 10m |
| $N_p$ = 35 cables | $A_r$ = 36m$^2$ |
| $W_p$ = 7.0kN/node | $(I_r)_p$ = 492m$^4$ |
| $D_p$ = 0.070m | $(E_r)_p$ = 34,000,000kNm$^2$ |
| $A_p$ = 0.003848m$^2$ | $(E_rI_r)_p$ = 17,000,000,000kNm$^2$ |
| $f = L_p/30$ = 6m | |
| $E_p$ = 200,000,000kN/m$^2$ | |
| $(EA)_p$ = 770,000kN | |
| $P_p$ = 800kN | |
| $(T_u)_p$ = 1,800kN | |

## 8 EXAMPLE 2

For the second example the prototype is a cable net with the characteristics given in Table 5, with different sag-to-span ratio from the model.

In order to have the parameters within the range of the charts we take:

$$E_m = \frac{E}{1.6} = \frac{200{,}000{,}000}{1.6}$$

Using 'eqns (12–25)' the prototype parameters can be scaled to the model, for which the above charts have been produced. Therefore:

$$\frac{L_m}{L_p} = \frac{100}{180} = 0.555 \qquad \frac{N_p + 1}{N_m + 1} = \frac{35 + 1}{25 + 1} = 1.385$$

$$\frac{E_m}{E_p} = \frac{200{,}000{,}000}{1.6 * 200{,}000{,}000} = \frac{1}{1.6}$$

$$\frac{(E_r)_m}{(E_r)_p} = \frac{34{,}000{,}000}{34{,}000{,}000} = 1$$

$W_m = W_p*(1/1.6)*1*0.555^2*1.385^2*(30/20)^{1/2}$ = 3.166kN/node

$D_m = 0.070*0.555*(1.385*1)^{1/2}*20/30 = 0.03048$m

$A_m = 0.003848*0.555^2*1.385*1*(20/30)^2$ = 0.0007296m$^2$

$(EA)_m = 770{,}000*(1/1.6)*1*0.555^2*1.385*(20/30)^2$ = 91,248.128kN

$P_m = 800*(1/1.6)*1*0.555^2*1.385 = 213$kN

$(T_u)_m = 1{,}800*(1/1.6)*1*0.555^2*1.385 = 480$kN

$b_m = 10*0.555*(1/1.6)^{1/4} = 4.93$m

$(I_r)_m = 492*0.555^4*(1/1.6) = 29.18$m$^4$

$(E_rI_r)_m = 17{,}000{,}000{,}000*(1/1.6)*1*0.555^4$ = 1,000,000,000kNm$^2$

For load $W_m$ = 3.166kN/node, stiffness of cables $(EA)_m$ = 100,000kN, pretension of cables $P_m$ = 213kN, and stiffness of the edge ring $(E_rI_r)_m$ = 1,000,000,000kNm$^2$, the values of maximum nodal deflection and maximum cable tension can be derived from chart a of Figure 10:

$d_m$ = 0.515m :maximum nodal deflection

$T_m$ = 315kN :maximum cable tension

These values can be scaled back to the prototype using the inverse 'eqns (17–18)':

$T_p = 315*1*1.6*1.8^2*0.722 = 1{,}180$kN

$d_p = 0.515*1.80 = 0.927$m

The values of maximum deflection and maximum internal forces of the edge ring as well as the maximum ring's deformations can be derived from charts a of Figures 12, 14 and 16:

$(N_x)_m$ = 3,700kN :maximum ring normal force

$(Q_y)_m$ = 1,500kN :maximum ring shear force

$(M_z)_m$ = 30,000kNm :maximum ring moment

$(d_x)_m$ = 0.022m :maximum ring deformation x

$(d_y)_m$ = 0.021m :maximum ring deformation y

These values can be scaled back to the prototype using the inverse 'eqns (22–25)' given in section 4 of

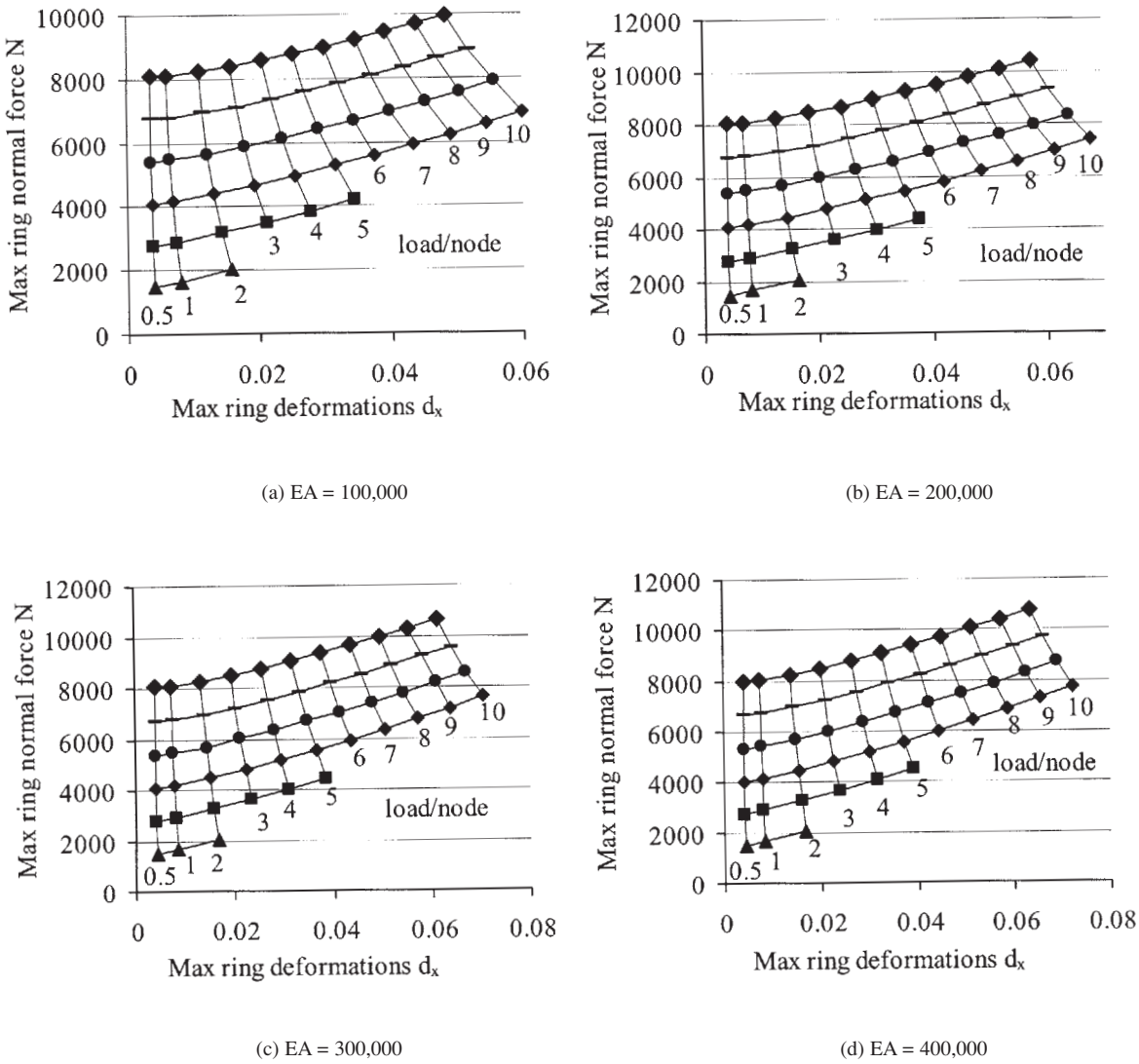


(a) EA = 100,000

(b) EA = 200,000

(c) EA = 300,000

(d) EA = 400,000

Figure 12. Charts of ring normal force $N_x$ and ring deformations $d_x$ for pretension P = 100–600, load per node W = 0.5–10, ring stiffness $E_rI_r$ = 1,000,000,000, cable stiffness EA = 100,000 ~ 400,000

this paper:

$(N_x)_p = 3{,}700*1*1.6*1.8^2 = 19{,}181\text{kN}$

$(d_x)_p = 0.022*1.8 = 0.0394\text{m}$

$(Q_y)_p = 1{,}500*1.6*1.8^2 = 7{,}776\text{kN}$

$(d_y)_p = 0.021*1.8 = 0.0378\text{m}$

$(M_z)_p = 30{,}000*1.6*1.8^3 = 279{,}936\text{kNm}$

Using the program SOFiSTiK and performing an exact nonlinear analysis of the prototype, the maximum deflection obtained for the nodes of the net is d = 0.945m and the maximum tension of the cables T = 1242kN, while the maximum internal forces and deformations obtained for the edge ring are:

$N_x = 21{,}393.63\text{kN}$

$d_x = 0.043\text{m}$

$Q_y = 8{,}206.341\text{kN}$

$d_y = 0.041\text{m}$

$M_z = 280{,}293.5\text{kNm}$

Thus, the accuracy is 98.1% for the net deflections, 95.0% for the cable tensions, 89.7% for the ring normal force $N_x$, 94.8% for the ring shear force $Q_y$,

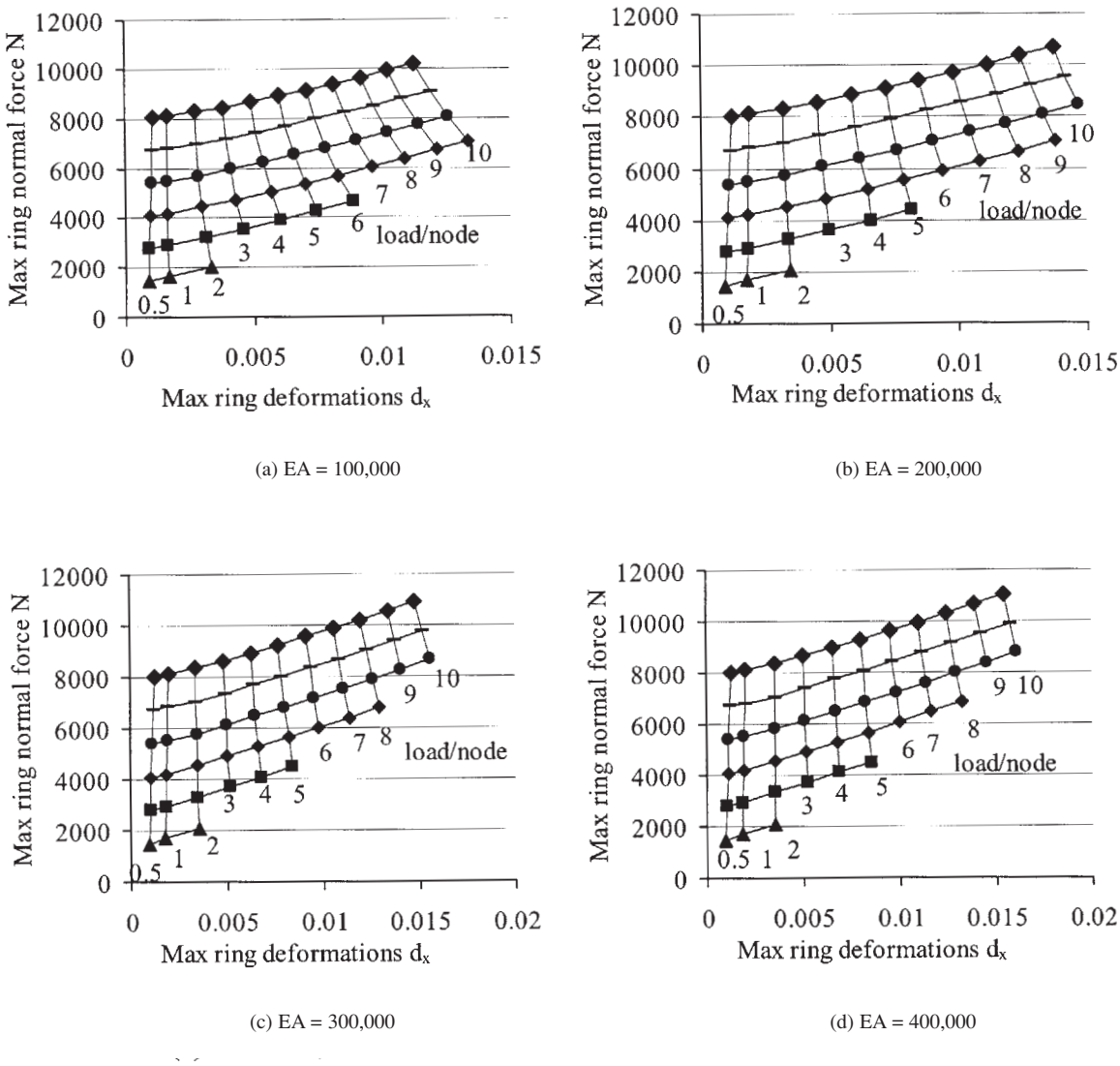


Figure 13. Charts of ring normal force $N_x$ and ring deformations $d_x$ for pretension P = 100–600, load per node W = 0.5–10, ring stiffness $E_rI_r$ = 5,000,000,000, cable stiffness EA = 100,000 ~ 400,000

99.9% for the ring moment $M_z$ and 91.6% and 91.7% for the ring deformations $d_x$ and $d_y$, respectively.

## 9 SUMMARY AND CONCLUSIONS

The behavior of cable net structures with elastic supports has been examined and a method of preliminary analysis of such systems has been presented and verified. It is possible to conclude that:

- The interaction between the edge ring and the cable net is significant. The edge ring cannot be neglected in the analysis of cable net structures, because its deformability causes considerable variations in the tensions of the cables and, particularly, in the deflections of the net. It cannot be analysed separately from the net either, because, in consequence to the nonlinear behavior of the cables, the response of the ring is also nonlinear.
- On the basis of the examples presented here, in which model and prototype have the same or different sag to span ratios, as well as numerous other examples, the proposed methodology of preliminary analysis of cable nets anchored to an elastically deformable edge ring gives satisfactory results for the estimation of the response of the system, both the cables and the edge ring, at a preliminary design stage.

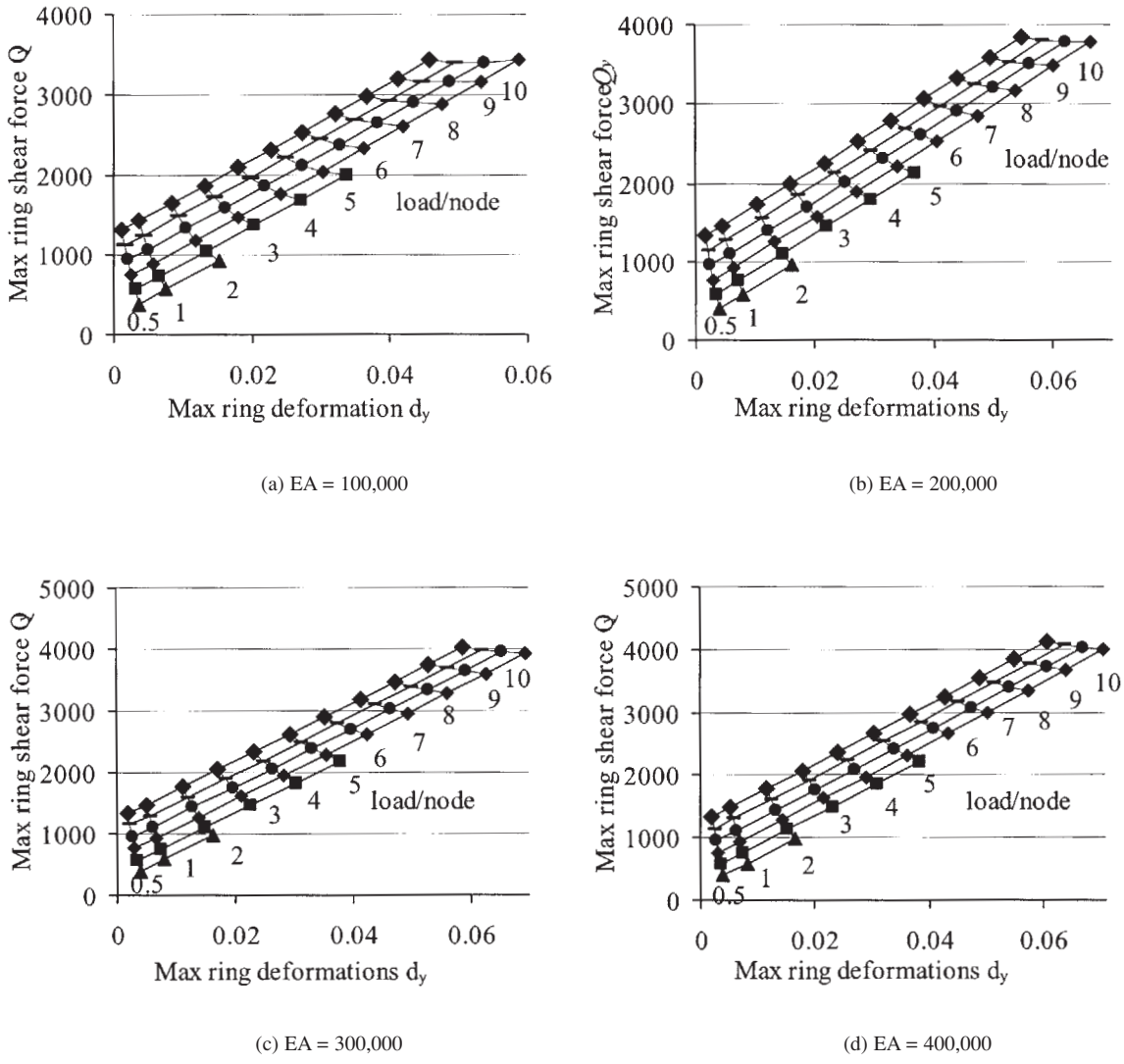


(a) EA = 100,000

(b) EA = 200,000

(c) EA = 300,000

(d) EA = 400,000

Figure 14. Charts of ring normal force $Q_y$ and ring deformations $d_y$ for pretension P = 100–600, load per node W = 0.5–10, ring stiffness $E_rI_r$ = 1,000,000,000, cable stiffness EA = 100,000 ~ 400,000

## REFERENCES


1. Buchholdt, H. A., *An introduction to cable roof structures*, Thomas Telford, London,1999.
2. Vilnay, O. *Cable nets and tensegric shells – Analysis and design applications* Technion – Israel Institute of Technology, Haifa, Israel, 1990.
3. Broughton, P. and Ndumbaro, P., *The analysis of cable and catenary structures*, Thomas Telford, London,1994.
4. Szabó, J., Kollár, L. and Pavlovic, M. V., *Structural design of cable-suspended roofs*, Akadémiai Kiadó, Budapest, Hungary and Ellis Horwood Limited, Chichester, England, 1984.
5. Majowiecki, M., *Tensostrutture Progetto e Verifica*, edizioni CREA, Italy (in italian), 1994.
6. Gero, J. S., Structures Report SR8, *The behaviour of cable network structures*, University of Sydney, 1975.
7. Gero, J. S., Structures Report SR9, *The preliminary design of cable network structures*, University of Sydney, 1975.
8. Giles, R. V., *Schaum's outline of theory and problems of fluid mechanics and hydraulics*, McGraw-Hill, New York, 1977.
9. Talvik, I., Finite element modeling of cable networks with flexible supports, *Computers and Structures* 79, 2001, pp. 2443–2450.
10. Majowiecki, M. and Zoulas, F. On the elastic interaction between the rope net and space frame anchorage structures in: Nooshin H, ed., *Proceedings of the International Conference on Space Structures*, University of Surrey, Guildford, UK.1984, 778–784.
11. SOFiSTiK version 4.2.00 (2000), SOFiSTiK AG – Structural Engineering Software, München.
12. Wikipedia, http://www.wikipedia.org/wiki/Buckingham_Pi_theore

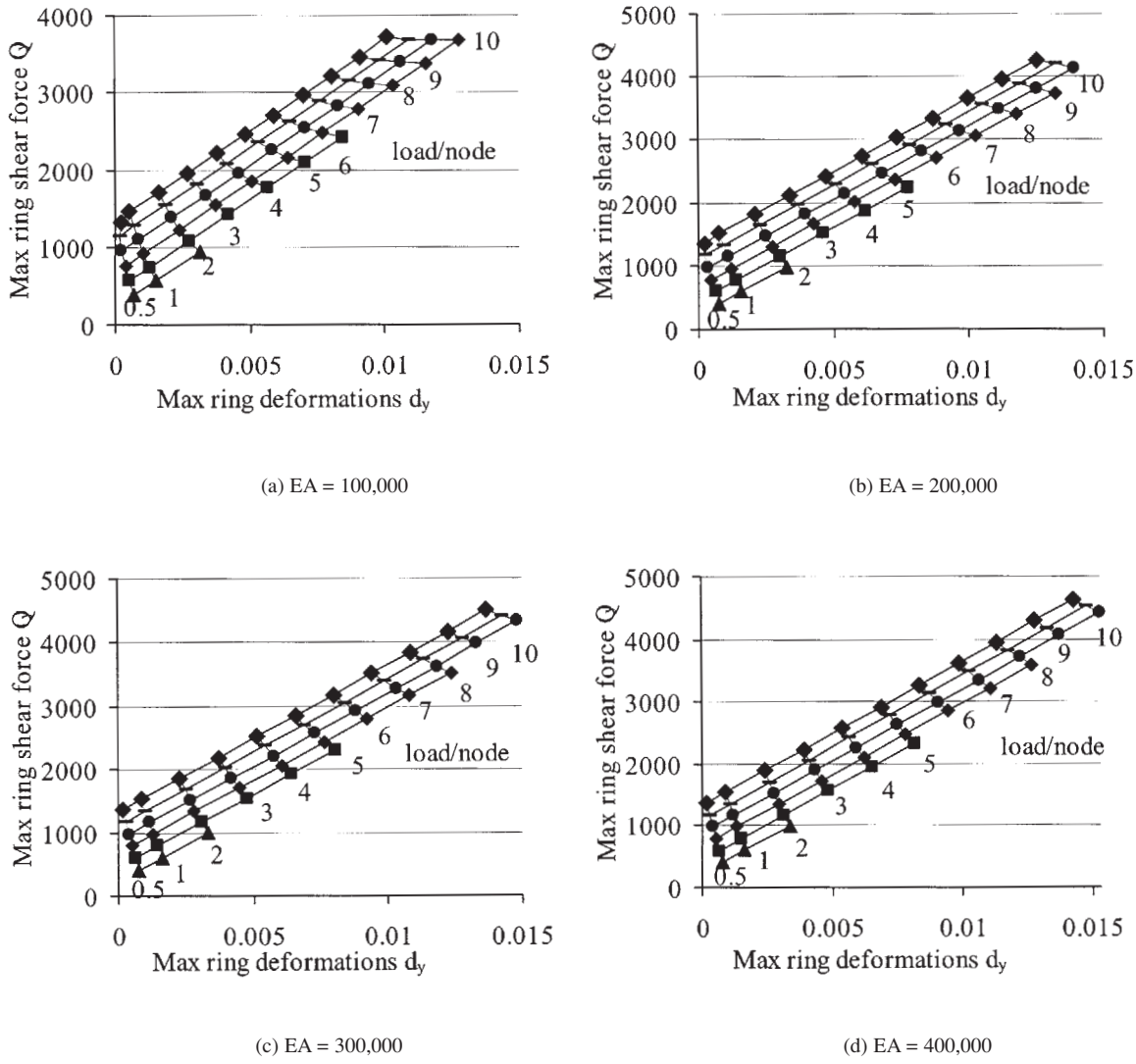


Figure 15. Charts of ring normal force $Q_y$ and ring deformations $d_y$ for pretension P = 100–600, load per node W = 0.5–10, ring stiffness $E_rI_r$ = 5,000,000,000, cable stiffness EA = 100,000 ~ 400,000

m, 2002.

13. Shih, C., *Buckingham Pi Theorem*, http://www.eng.fsu.edu/~shih/eml3016/lecture-notes/buckingham%20pi%20theorem/sld001.htm, 2000.
14. Vassilopoulou, I., Gantes, C. J., Behaviour and preliminary analysis of cable net structures with elastic supports, in: Beskos, D.E., Karabalis, D.L., Kounadis, A.N., eds., *Proceedings of the 4th National Conference on Steel Structures (vol. 2)*, Patras, Greece, 2002, 517–525.
15. Vassilopoulou, I., Gantes, C. J. (2004) Behavior, Analysis and Design of Cable Networks Anchored to a Flexible Edge ring, in: Motro, R. ed., *International Association for Shell and Spatial Structures, Proceedings of the IASS Symposium on Shell and Spatial Structures from Models to Realization*, Montpellier, France, 2004, Extended Abstract, pp. 212–213.
16. Vassilopoulou, I., *Behavior and analysis of cable net roofs*, Graduate Degree Thesis Civil Engineering Department, National Technical University of Athens (in greek ), 2001.

## NOTATION

The following symbols are used in this paper:

A = cable cross sectional area;
$A_r$ = edge ring sectional area;
b = ring cross section width;
D = cable diameter;
d = nodal deflections;
$d_r$ = ring deformation;
$d_x$ = ring deformation in the global x-direction;
$d_y$ = ring deformation in the global y-direction;
E = elastic modulus of cable material;
$E_r$ = elastic modulus of ring material;

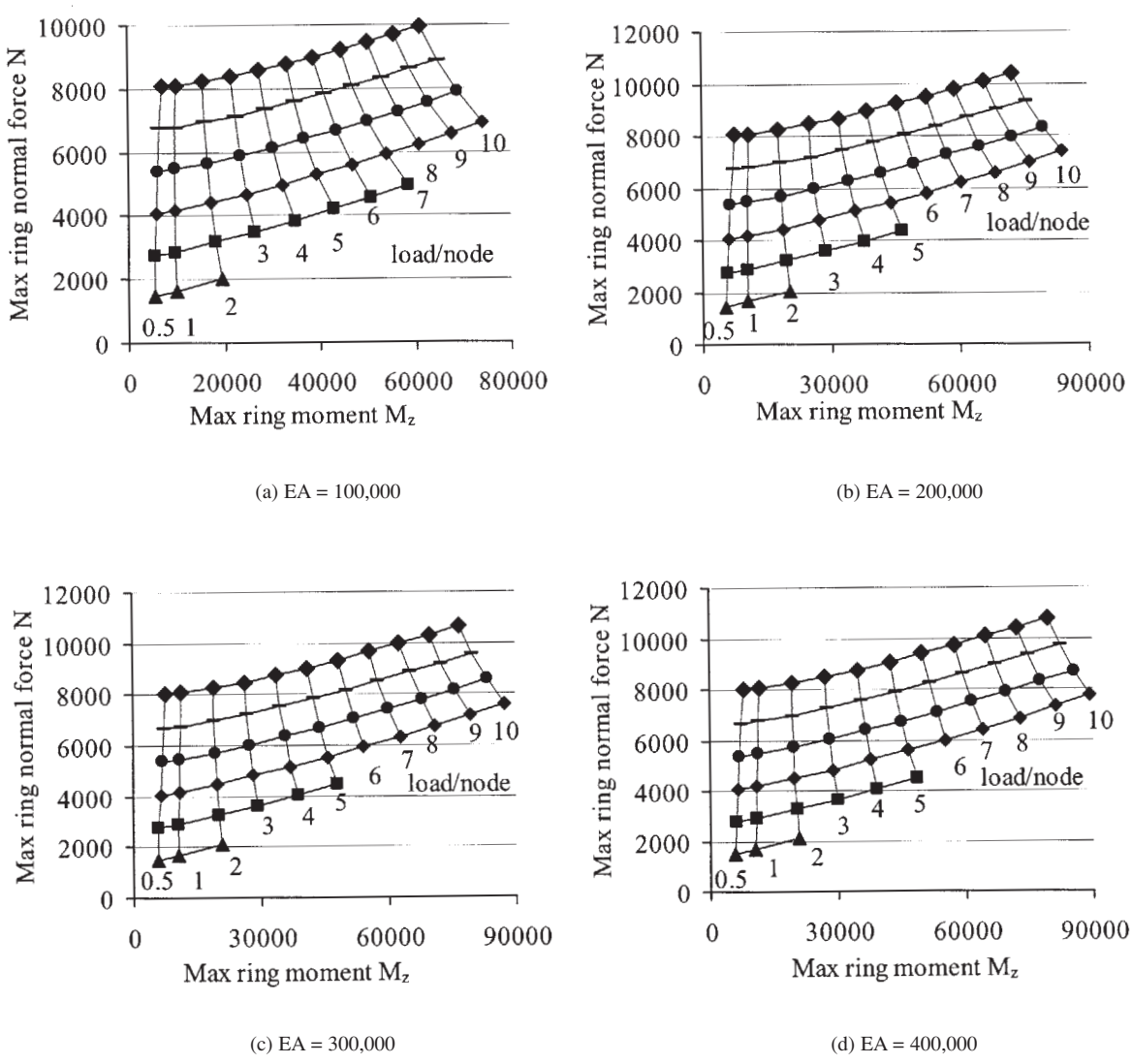


(a) EA = 100,000

(b) EA = 200,000

(c) EA = 300,000

(d) EA = 400,000

Figure 16. Charts of ring normal force $N_x$ and ring deformations $M_z$ for pretension P = 100–600, load per node W = 0.5–10, ring stiffness $E_rI_r$ = 1,000,000,000, cable stiffness EA = 100,000 ~ 400,000

EA = cable axial stiffness;
$E_rI_r$ = ring flexural stiffness;
f = sag of the circular cable net plan view;
$f_x$ = sag of the elliptical cable net plan view in the x-direction;
$f_y$ = sag of the elliptical cable net plan view in the y-direction;
$I_r$ = ring moment of inertia;
$k_x$ = curvature of the elliptical cable net plan view in the x-direction;
$k_y$ = curvature of the elliptical cable net plan view in the y-direction;
L = diameter of circular cable net plan view;
$L_x$ = diameter of elliptical cable net plan view in the x-direction;
$L_y$ = diameter of elliptical cable net plan view in the y-direction;
$M_y$ = ring bending moment in the local y-direction;
$M_z$ = ring bending moment in the local z-direction;
N = number of cables per direction;
$N_x$ = ring normal force;
P = cable pretension;
$Q_y$ = ring shear force in the local y-direction;
$Q_z$ = ring shear force in the local z-direction;
T = cable tension;
$T_u$ = cable ultimate tensile strength;
W = nodal loads;
x = x-coordinate of the cable net;
y = y-coordinate of the cable net; and
z = z-coordinate of the cable net.

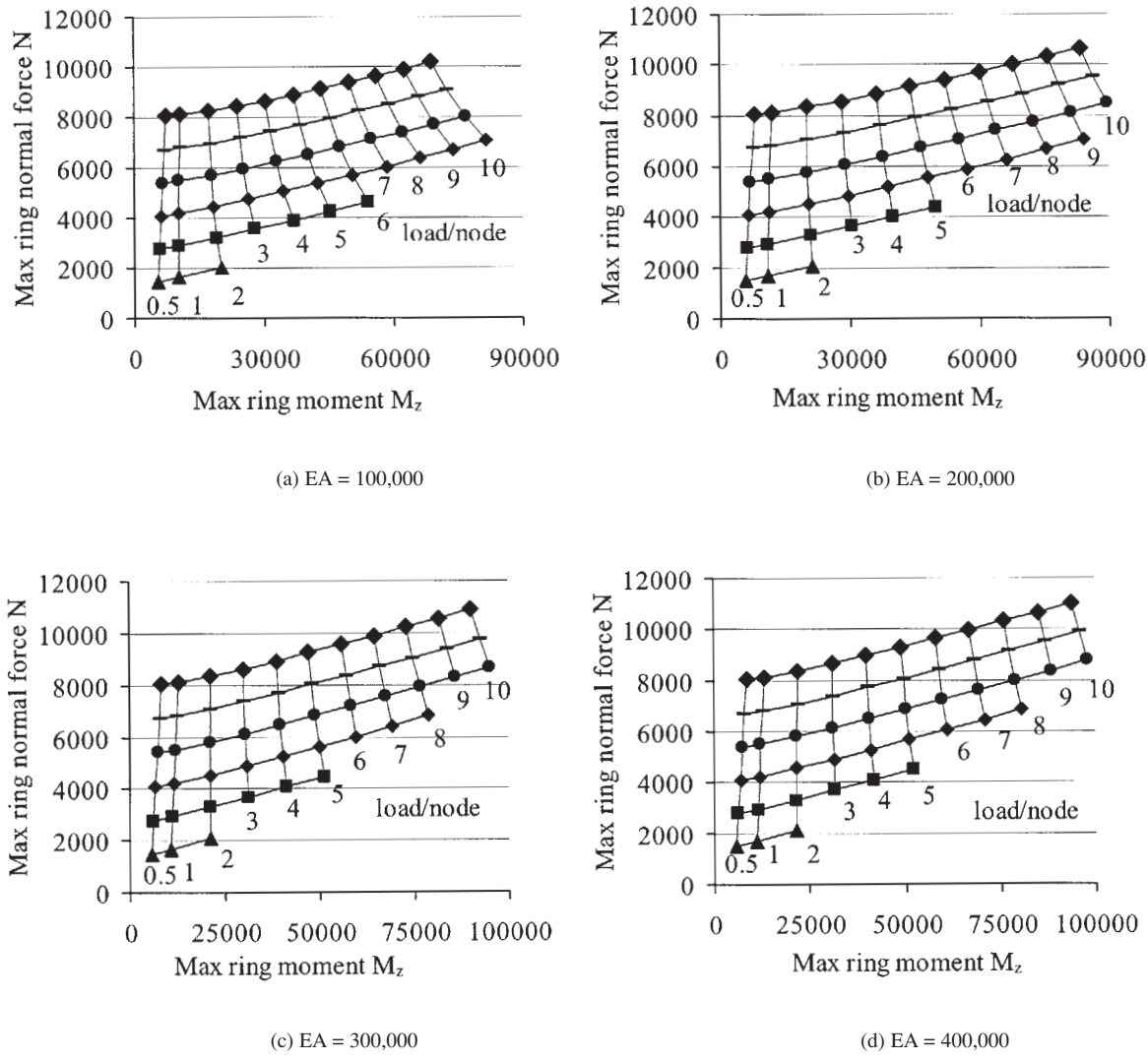


Figure 17. Charts of ring normal force $N_x$ and ring deformations $M_z$ for pretension P = 100–600, load per node W = 0.5–10, ring stiffness $E_rI_r$ = 5,000,000,000, cable stiffness EA = 100,000 ~ 400,000

**Subscripts**

m = model;
p = prototype; and
r = edge ring.